CORROSION SCIENCE AND TECHNOLOGY, Vol.31, No.6(2002), pp.438~443

XPS and Electrochemical Studies of Amorphous Ni-Nb-Ta-P Alloys in 12 M HCl

A. Kawashima, T. Sato*, and K. Asami*

The Oarai Branch, Institute for Materials Research, Tohoku University
Oarai Ibaraki, 311-1313 Japan
**Institute for Materials Research, Tohoku University,*
Sendai, 980-8577 Japan

The open circuit potentials of the amorphous Ni-Nb-Ta-P alloys containing 15 at% or more tantalum increased with immersion time and are located in the passive region of the alloys, although those with containing 10 at% or less tantalum decrease with immersion time in 12 M HCl solution at 30°C open to air. The high tantalum-bearing alloys are spontaneously passivated. XPS analysis revealed that the spontaneous passive films formed on the alloys in the hydrochloric acid are rich in tantalum and niobium cations and deficient in nickel cation. The high corrosion resistance of these alloys with high tantalum content is attributed to the protective nature of passive film consisting of hydrated tantalum oxyhydroxide.

Keywords *: amorphous Ni-Nb-Ta-P alloys, XPS, passive film, passivity*

1. Introduction

Since melt spun amorphous Fe-Cr-P-C alloys with extremely high corrosion resistance were discovered in 1974.[1] a number of corrosion-resistant amorphous alloys were prepared.[2),3)] They have, however, been mostly fabricated as thin ribbons or films less than a millimeter in thickness. Because of their limited thickness, it is difficult to use corrosion-resistant amorphous alloys in practical service.

Recently, a several families of multi-component metallic alloys exhibiting excellent glass-forming ability have been developed.[4),5)] Although mechanical and magnetic properties of the bulk amorphous alloys have extensively studied, little attention has been paid to the corrosion behavior of the alloys and to tailoring corrosion-resistant bulk amorphous alloys.

Nickel-based alloys are important engineering materials. However, there have been no data on the synthesis and properties of nickel-based bulk amorphous alloys, except for our work.[6-8)] We have recently reported that bulk amorphous Ni-Nb-Ta-P[7)] alloys were obtained in a wide composition range by a copper mold casting. Their corrosion resistance increases with an increase in tantalum content. The bulk amorphous $[Ni-(40-x)Nb-xTa]_{0.95}-5P$ alloys with x = 20-40 at.% are spontaneously passive, and are immune to corrosion even in 12 M HCl open to air at 30°C. The corrosion behavior of the bulk alloys is almost the same as corresponding melt-spun amorphous alloy ribbons. In the present work, XPS was used to investigate the composition of the surface films formed on the melt-spun amorphous Ni-Nb-Ta-P alloy ribbons immersed in the 12 M HCl to elucidate the origin of the high corrosion-resistance of the corresponding new bulk amorphous alloys.

2. Experimental

The alloy series $[Ni-(40-x)Nb-xTa]_{0.95}-5P$ (x=0, 5, 10, 15, 20, 25, 30, 35, 40 at %) was chosen. Alloy ingots were prepared by arc melting of nickel phosphide, nickel, tantalum and niobium under an argon atmosphere. The amorphous alloy ribbons approximately 2 mm wide and 20 μm were prepared by a melt spinning method in the argon atmosphere. The amorphous structure was confirmed by the X-ray diffraction method using Cu K_α radiation. Prior to immersion and electrochemical measurements alloy specimens were polished mechanically with silicon carbide paper up to No 1500 in cyclohexane, degreased with aceton and dried in air.

Potentiodynamic polarization curves were measured in 12 M HCl solution at 30°C open to air with a potential sweep rate of 50 mV min^{-1}. For the measurement of potentiodynamic polarization curves, potentials were swept

from the corrosion potential after immersion for 30 min in the anodic or cathodic direction. The reference electrode used was a saturated calomel electrode (SCE). The open circuit potential was also measured as a function of time.

Before and after open circuit immersion in the solution, XPS spectra from the alloy specimens were measured by using SSI SSX-100 photoelectron spectrometer with Al K_α excitation ($h\nu$ = 1486.6 eV). Binding energies of electrons were determined by a calibration method described elsewhere.[9),10)] The composition and thickness of surface film and the composition of the substrate alloy immediately under the surface film were quantitatively determined by a previously proposed method, using integrated intensities of spectra.[11)] The photo-ionization cross-sections of the Ni $2p_{3/2}$, Ta 4f, Nb $3d_{5/2}$, and P 2p electrons relative to the O 1s electrons used were 2.32,[12)] 2.62,[13)] 2.98[14)] and 0.79,[15)] respectively.

3. Results and discussion

3.1 Structure of the alloys

X-ray diffraction patterns of the melt-spun [Ni-(40-x) Nb-xTa]$_{0.95}$-5P alloys are shown in Fig. 1. All of the alloys show halo patterns typical of amorphous structure. The alloys of x = 5, 15, 25, 35 showed similar halo patters.

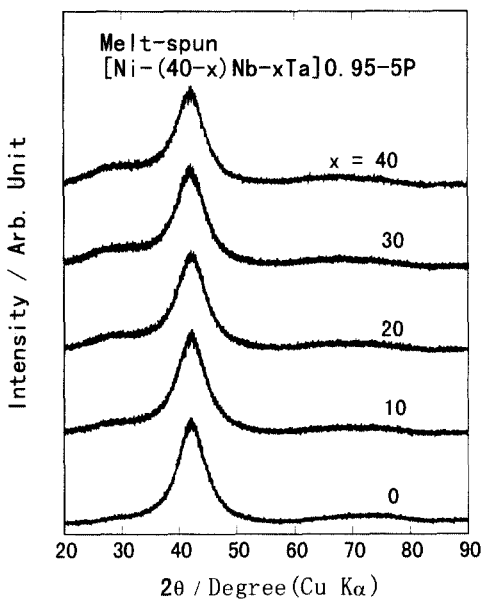

Fig. 1. XRD patterns for melt-spun [Ni-(40-x)Nb-xTa]$_{0.95}$-5P alloys

3.2 Open circuit potential and polarization behavior

Fig. 2 shows the change in the open circuit potential as a function of time for the melt-spun amorphous alloys

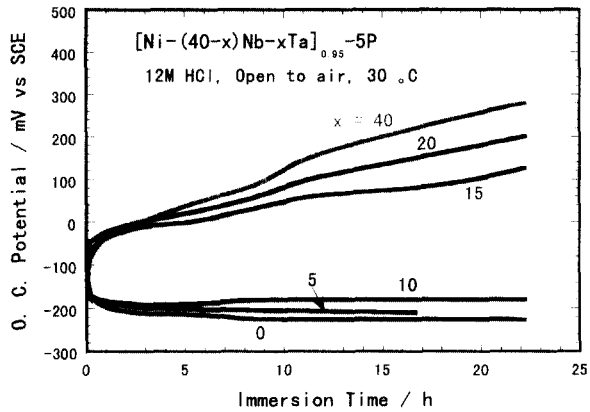

Fig. 2. Change in open circuit potentials for melt-spun [Ni-(40-x)Nb-xTa]$_{0.95}$-5P alloys in 12M HCl solution open to air at 30℃ as a function of immersion time.

in a 12M HCl solution open to air at 30℃. The open circuit potential of commercially pure tantalum is also shown for comparison, and is about -120 mV just after immersion, increases up to about 0 mV within about 5 h, and then increases slightly with immersion time. The open circuit potentials of the alloys containing 15 at% or more tantalum are also about -120 mV just after immersion, increase rapidly within 1 h immersion and further increase gradually with immersion time and with alloy tantalum content. They become higher than that of tantalum and are located in the passive region of tantalum, similarly to the other tantalum containing alloys.[13),16)] Accordingly, the alloys containing 15 at% or more tantalum are passivated spontaneously in agreement with high corrosion resistance in the aggressive concentrated hydrochloric acid.[7)] In contrast to these alloys, the open circuit potentials for the alloys with 10 at% or less tantalum decrease rapidly down to about -190 mV within 1 h and stay at low potentials from -180 to -210 mV depending on alloy tantalum content and are located in the active region of the alloys. In fact, after immersion for 6 days the alloys with 15 at% or more tantalum maintained metallic luster but those with lower tantalum content were covered with black-colored corrosion product film within 2 h immersion. This fact indicates that the addition of a certain amount of tantalum is effective for the ennoblement of the open circuit potential, and hence for high corrosion resistance.

Fig. 3 shows the potentiodynamic polarization curves of the melt-spun amorphous alloys measured in the 12M HCl open to air at 30 ℃ after immersion for 30 min. Included in this Fig. for comparison is that for tantalum metal. The polarization behavior mainly changes with alloy tantalum content. The amorphous alloys containing 10 at% or less tantalum shows the active-passive transition

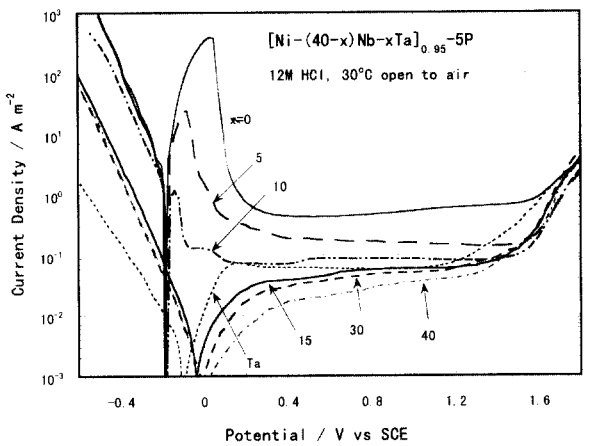

Fig. 3. Potentiodynamic polarization curves for melt-spun [Ni-(40-x)Nb-xTa]$_{0.95}$-5P alloys measured in 12M HCl solution open to air at 30 ℃, including tantalum metal

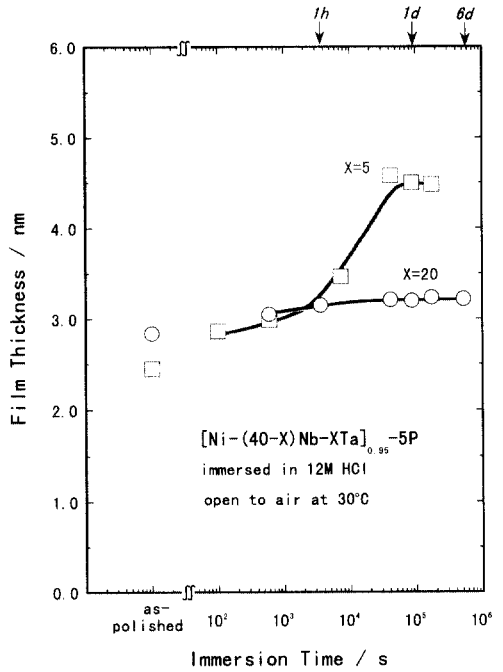

Fig. 4. Film thickness formed on the amorphous (Ni-35Nb-5Ta)$_{0.95}$-5P and (Ni-20Nb-20Ta)$_{0.95}$-5P alloys after mechanical polishing and immersion in 12M HCl solution open to air at 30 ℃ as a function of immersion time.

and the passive current densities are relatively high. An increase in the tantalum content leads to ennoblement of the open circuit potential and decrease in the current densities both the active and passive states. The alloys containing 15 at% or more tantalum are ennobled to the passive region of tantalum, because of a decrease in the anodic current density along with the increase in cathodic current density, and are spontaneously passivated and their passive current densities are lower than that of tantalum metal. These changes with the tantalum content are in accordance with results of corrosion rates test for these alloys in 12 M HCl.[7]

All the alloys containing tantalum show a wide passive region up to transpassive region of nickel and a no steep increase in current density due to pitting dissolution during anodic polarization. In the transpassive region, the current densities for all the alloy specimens become the same as each other.

3.3 XPS analysis of surface film

The corrosion behavior under the open circuit condition was further examined by XPS analysis of the surface film for high corrosion-resistant (Ni-20Nb-20Ta)$_{0.95}$-5P and poor corrosion-resistant (Ni-35Nb-5Ta)$_{0.95}$-5P alloy specimens. XPS spectra from the alloys exhibited peaks of nickel, niobium, tantalum, phosphorus, oxygen, chlorine and carbon. The C 1s peak arose from a contaminant hydrocarbon layer covering the specimen surface. Cl 2p peak was assigned to Cl^- ion in the surface film, but the concentration of Cl^- ion was negligibly small. Ni $2p_{3/2}$ spectra consisted of two peaks at about 853.0 and 856.3 eV, corresponding to the metallic and the Ni^{2+} states, respectively.[17] However, the intensity of the spectra for nickel ion in the surface film was quite low, in contrast to those of niobium and tantalum ions. The Nb 3d spectra consisted of two sets of doublet peaks corresponding to $3d_{5/2}$ and $3d_{3/2}$ peaks of metallic and oxidized states. The peak observed at 207.1-207.8 eV was assigned to Nb 3d electrons of Nb^{5+} ions in the surface film and that at 202.7-203.1 eV to Nb 3d electrons of the metallic state of niobium in the alloy under the surface films.[14] The Ta 4f spectra also consisted of two sets of doublet peaks corresponding to $4f_{7/2}$ and $4f_{5/2}$ peaks of metallic and oxidized states. The peak observed at 26.0-26.7 eV was assigned to Ta $4f_{5/2}$ electrons of Ta^{5+} ions in the surface film and that at 22.2-22.8 eV to Ta 4f electrons of the metallic state of tantalum.[13] The signals of P 2p electrons in the oxidized and metallic states were observed at the binding energy of about 132.9 and 129.5 eV, respectively. Phosphorus in the surface film was assigned to be pentavalent phosphorus.[18] The O 1s spectrum showed a peak at about 531.4 eV and a large full width at half maximum because of overlap of O 1s spectra from O^{2-}, OH^-, PO_4^{3-} and H_2O, although they were not separated into four peaks in this work.

Fig. 4 shows the change in thickness of the surface film formed on the alloys with immersion time. The thickness of the air-formed film is also shown for comparison. The thickness of air-formed film formed on (Ni-35Nb-5Ta)$_{0.95}$-5P alloy is about 2.5 nm and largely increases after immersion

for 1 h, in accordance with formation of corrosion product film. After two days immersion, 5Ta alloy ribbon became extremely embrittled by hydrogen, absorbed during dissolution, XPS measurement could not be carried out. By contrast, the film thickness of air-formed film formed on the $(Ni\text{-}20Nb\text{-}20Ta)_{0.95}\text{-}5P$ alloy is about 2.8 nm, and after immersion for 10 min film thickness slightly increases up to about 3.0 nm, and after 1 h it becomes about 3.1 nm and keeps almost same value for prolonged immersion for 6 days. These facts indicate that the film formed on the 20Ta alloy is highly dense and stable even in this aggressive acid.

Fig. 5 shows the cationic fraction in the spontaneously passive film and the atomic fraction in the underlying alloy surface for amorphous $(Ni\text{-}20Nb\text{-}20Ta)_{0.95}\text{-}5P$ as a function of immersion time in 12M HCl solution open to air at 30 ℃. The composition of air-formed film on the alloy is also shown for comparison. As shown in Fig. 5(a), cationic fractions of both tantalum and niobium for the air-formed film are almost the same value of about 0.39, while atomic fractions of tantalum and niobium are almost the same value of about 0.15, shown in Fig. 5(b). Accordingly, the concentration of both tantalum and niobium ions in the air-formed film are significantly higher than those of the alloy itself, while both tantalum and niobium are deficient in the underlying alloy surface just below the surface film, as shown Fig. 5 (b). This fact indicates the preferential oxidation of tantalum and niobium in air exposure after/during mechanical polishing. Nickel is largely deficient in the air-formed film, while it is slightly enriched in the underlying alloy surface, and phosphorus virtually does not exist in the air formed film. The enrichment of nickel in the underlying alloy surface is reasonable because nickel in the alloy is not oxidized by air exposure.[19]

When the 20 Ta alloy is immersed in the solution, further enrichment of tantalum in the passive film takes place and the tantalum content gradually increases with immersion time due to the rapid dissolution of nickel from the surface film. The cationic fraction of tantalum of 0.47 after 10 min immersion increases up to 0.55 for prolonged immersion of 6 days. The concentration of niobium ion in the surface film decreases slightly with immersion time, but it is still much higher than that of alloy itself even after 6 days immersion. Furthermore, as shown in fig.5 (b), atomic fractions of the alloy becomes almost the same as those of the alloy itself after initial immersion and remained unchanged during prolonged immersion, indicating the high stability of the alloy. From these results, it can be said that the fast conversion of the air-formed film to stable passive film enriched in tantalum and

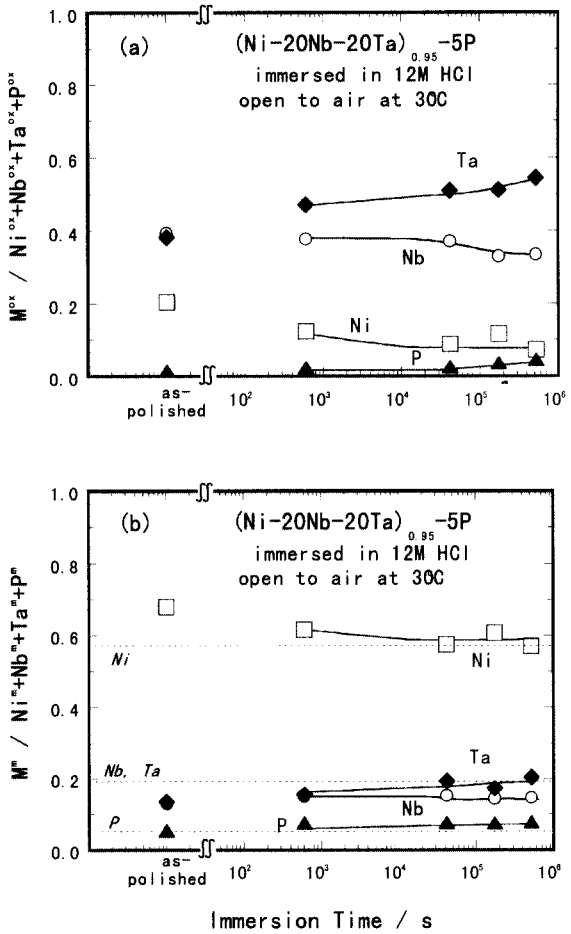

Fig. 5. (a) Cationic fraction in the surface film and (b) atomic fraction in the underlying alloy surface for the amorphous $(Ni\text{-}20Nb\text{-}20Ta)_{0.95}\text{-}5P$ alloy in 12M HCl solution open to air at 30 ℃ as a function of immersion time.

niobium occurs on the alloy. The formation of oxyhydroxide film composed of mainly tantalum and niobium seems to be responsible for the high corrosion resistance of the high tantalum-bearing alloys in the concentrated hydrochloric acid.

In contrast to high tantalum-bearing alloys, a stable passive film cannot be formed for the low tantalum bearing alloys. Figs. 6 (a) and (b) show the change in the cationic fraction in the surface film and the atomic fraction in the underlying alloy surface, respectively, for the low tantalum amorphous $(Ni\text{-}35Nb\text{-}5Ta)_{0.95}\text{-}5P$ alloy as a function of immersion time in 12M HCl solution open to air at 30 ℃. In the air-formed film, the enrichment of both tantalum and niobium in the film occurs due to the similar manner as the high tantalum-bearing alloy shown in Fig. 5. Open circuit immersion in 12 M HCl leads to rapid dissolution of nickel from the surface film with a consequent increase in niobium and tantalum content. Concentration of the

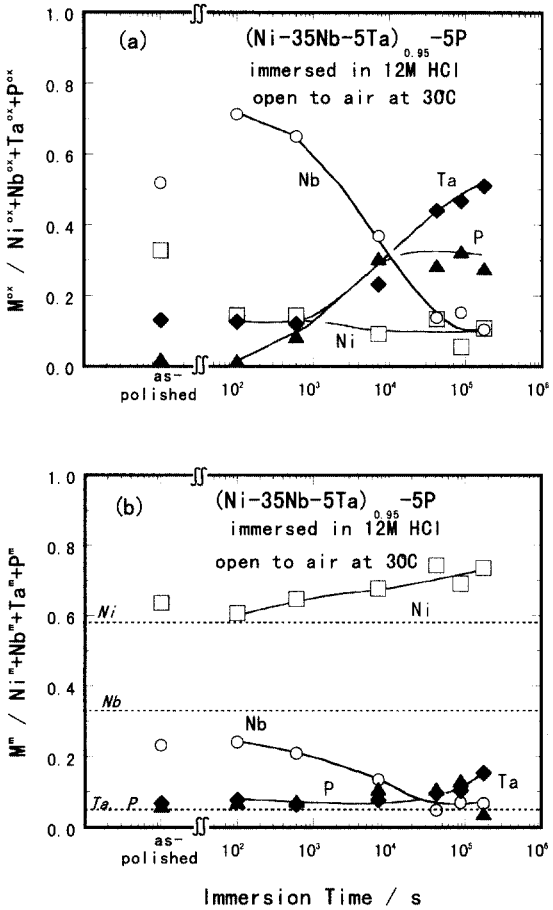

Fig. 6. (a) Cationic fraction in the surface film and (b) atomic fraction in the underlying alloy surface for the amorphous $(Ni\text{-}35Nb\text{-}5Ta)_{0.95}$-5P alloy in 12M HCl solution open to air at 30 ℃ as a function of immersion time.

tantalum and the phosphorus cations in the film significantly increases with immersion time due to dissolution of niobium and nickel, while tantalum and niobium in the underlying surface are deficient. Taking into account the facts that the amorphous $(Ni\text{-}35Nb\text{-}5Ta)_{0.95}$-5P alloy dissolved actively and the alloy surface became black during immersion of 5 h, the increase in tantalum and phosphorus content in the film on the $(Ni\text{-}35Nb\text{-}5Ta)_{0.95}$-5P alloy with immersion time is attributable to accumulation of corrosion products with low solubility, such as tantalum phosphate, on the alloy surface as a result of continuous corrosion.

Accordingly, a certain amount of tantalum addition is quite effective for the formation of a highly protective passive film in the aggressive hydrochloric acid.

4. Conclusions

The corrosion behavior of melt-spun amorphous Ni-Nb-Ta-P alloys in 12M HCl solution open to air at 30 ℃ was investigated by electrochemical and XPS measurements. The following conclusions are drawn:

1) The amorphous $[Ni\text{-}(40\text{-}x)Nb\text{-}xTa]_{0.95}$-5P alloys ($x \geqq 15$ at%) are spontaneously passivated in 12 M HCl. Their open circuit potentials are higher than that of tantalum metal. The low tantalum-bearing alloys ($x \leqq 10$ at%), however, show the active-passive transition.

2) The open circuit potentials of Ni-Nb-Ta-P alloys containing sufficient amount of tantalum are ennobled to the passive region of tantalum, because of a decrease in the anodic current density along with the increase in cathodic current density.

3) The spontaneous passive film formed on the tantalum-bearing alloys are rich in tantalum as well as niobium due to preferential dissolution of nickel. The high corrosion resistance of the alloys with sufficient amount of tantalum is ascribed to the formation of stable passive film consisting mainly of hydrated tantalum oxyhydroxide.

References

1. M. Naka, K. Hashimoto, and T. Masumoto, *J. Jpn. Inst. Met.*, **38**, 835 (1974).
2. H. Yoshioka, H. Habazaki, A. Kawashima, K. Asami, and K. Hashimoto, *Corros. Sci,*. **31**, 349 (1990).
3. J. H. Kim, E. Akiyama, H. Habazaki, A. Kawashima, K. Asami, and K. Hashimoto, *Corros. Sci*, **34**, 1947 (1993).
4. A. Inoue, K. Ohtera, K. Kita, and T. Masumoto, *Jpn. J. Appl. Phys.*, **27**, L2248 (1988).
5. A. Peker and W. L. Johnson, *Appl. Phys. Lett.*, **63**, 2342 (1993).
6. H. Habazaki, T. Sato, A. Kawashima, K. Asami, and K. Hashimoto, *Mater. Sci. Eng*, **A 304-306**, 696 (2001).
7. A. Kawashima, H. Habazaki, and K. Hashimoto, *Mater. Sci. Eng*, **A 304-306**, 753 (2001).
8. H. Katagiri, S. Meguro, M. Yamasaki, H. Habazaki, T. Sato, A. Kawashima, K. Asami, and K. Hashimoto, *Corros. Sci.*, **43**, 171 (2001) and **43**, 183 (2001).
9. K. Asami, J. Electron *Specrosc.*, **9**, 469 (1976).
10. K. Asami and K. Hashimoto, *Corros. Sci*, **17**, 559 (1977).
11. K. Asami, K. Hashimoto, and S. Shimodaira, *Corros. Sci.*, **17**, 713 (1977)..
12. E. Akiyama, H. Habazaki, A. Kawashima, K. Asami, and K. Hashimoto, *Mater. Sci. Eng*, **A 181/182**, 1128 (1994).
13. J. H. Kim, H. Yoshioka, H. Habazaki, A. Kawashima, K. Asami, and K. Hashimoto, *Corros. Sci,*. **33**, 1507 (1992).
14. E. Hirota, H. Yoshioka, H. Habazaki, A. Kawashima, K. Asami, and K. Hashimoto, *Corros. Sci,*. **32**, 1213 (1991).
15. K. Hashimoto, M. Kasaya, K. Asami, and T. Masumoto, *Boshoku Gijutsu (Corros. Engng)*, **26**, 445 (1977).

16. J. H. Kim, E. Akiyama, H. Habazaki, A. Kawashima, K. Asami, and K. Hashimoto, *Corros. Sci,*. **34**, 1947 (1993).
17. K. Asami, H. M. Kimura, K. Hashimoto, T. Masumoto, A. Yokoyama, H. Komiyama, and H. Inoue, *J. Non-Cryst. Solids*, **64**, 149 (1984).
18. M. Pelavin, D. N. herderickson, J. M. Hollander, and W. L. Jolly, *J. Phys. Chem.*, **74**, 1116 (1970).
19. X.-Y. Li, E. Akiyama, H. Habazaki, A. Kawashima, K. Asami, and K. Hashimoto, *Corros. Sci,*. **41**, 1095 (1999).